

# Statistics of opinion domains of the majority-vote model on a square lattice

Lucas R. Peres and José F. Fontanari

*Instituto de Física de São Carlos, Universidade de São Paulo,  
Caixa Postal 369, 13560-970 São Carlos, São Paulo, Brazil*

The existence of juxtaposed regions of distinct cultures in spite of the fact that people's beliefs have a tendency to become more similar to each other's as the individuals interact repeatedly is a puzzling phenomenon in the social sciences. Here we study an extreme version of the frequency-dependent bias model of social influence in which an individual adopts the opinion shared by the majority of the members of its extended neighborhood, which includes the individual itself. This is a variant of the majority-vote model in which the individual retains its opinion in case there is a tie among the neighbors' opinions. We assume that the individuals are fixed in the sites of a square lattice of linear size  $L$  and that they interact with their nearest neighbors only. Within a mean-field framework, we derive the equations of motion for the density of individuals adopting a particular opinion in the single-site and pair approximations. Although the single-site approximation predicts a single opinion domain that takes over the entire lattice, the pair approximation yields a qualitatively correct picture with the coexistence of different opinion domains and a strong dependence on the initial conditions. Extensive Monte Carlo simulations indicate the existence of a rich distribution of opinion domains or clusters, the number of which grows with  $L^2$  whereas the size of the largest cluster grows with  $\ln L^2$ . The analysis of the sizes of the opinion domains shows that they obey a power-law distribution for not too large sizes but that they are exponentially distributed in the limit of very large clusters. In addition, similarly to other well-known social influence model – Axelrod's model – we found that these opinion domains are unstable to the effect of a thermal-like noise.

PACS numbers: 89.75.Fb, 87.23.Ge, 05.50.+q

## I. INTRODUCTION

Despite the tendency of social actors to become more similar to each other through their local interactions [1, 2], global polarization, i.e., the existence of stable multicultural regimes, is a ubiquitous phenomenon in human society [3, 4]. This issue has been addressed by somewhat idealized agent-based simulations of human behavior producing highly nontrivial insights on the nature of the collective behavior that results from the homogenizing local interactions (see [5] for a recent review).

In this line, a particularly successful model is Axelrod's model for the dissemination of culture or social influence [6]. In Axelrod's model, the agents are placed at the sites of a square lattice of size  $L \times L$  and can interact with their nearest neighbors only. The culture of an agent is represented by a string of  $F$  cultural features, where each feature can adopt a certain number  $q$  of distinct traits. The interaction between any two neighboring agents takes place with probability proportional to the number of traits they have in common. Although the result of such interaction is the increase of the similarity between the two agents, as one of them modifies a previously distinct trait to match that of its partner, the model exhibits global polarization [6]. The key ingredient for the existence of stable globally polarized states in Axelrod's model is the rule that prohibits the interaction between agents which do not have any cultural trait in common. Relaxation of this rule so as to permit interactions regardless of the similarity between agents leads to one of the  $q^F$  distinct absorbing homogeneous configurations [7]. In addition, introduction of external noise so

that traits can change at random with some small probability [8], as well as the increase of the connectivity of the agents [9–11], destabilizes the polarized state also.

Although Axelrod's model enjoyed great popularity among the statistical physics community due mainly to the existence of a non-equilibrium phase transition [12] that separates the globally homogeneous from the globally polarized regimes [13, 14], the vulnerability of the polarized absorbing configurations was considered a major drawback to explaining robust collective social behavior. In this vein, Parisi et al. [15] have proposed a lattice version of the classic frequency bias mechanism for cultural or opinion change [3, 4], which assumes that the number of people holding an opinion is the key factor for an agent to adopt that opinion, i.e., people have a tendency to espouse cultural traits that are more common in their social environment. Actually, almost any model of cultural transmission admits that the probability that an individual acquires a cultural variant depends on the frequency of that variant in the population. The frequency-dependent bias mechanism requires, however, that the individual be *disproportionately* likely to acquire the more common variant [3].

More to the point, in the model of Parisi et al. the culture of an agent is specified by a binary string of length  $F$  (so  $q = 2$ ) and each bit of that string takes the value which is more common among its neighbors [15]. Since the model can be immediately recognized as  $F$  independent majority-vote models [16, 17], we found the claim by those authors that such model exhibits a polarized regime most intriguing. In order to check whether the multicultural absorbing configurations reported by Parisi et al. were not artifacts of the small lattice size used in

their study ( $L = 20$ ), in this paper we present a detailed analysis of the effects of the finite size of the lattice by considering square lattices of linear size up to  $L = 4000$ . In addition, we set  $F = 1$  to stress the identification with the well-known majority vote model of statistical physics. Hence the agents or sites of the lattices are modeled by Ising spins.

Our findings indicate that the polarized regime is indeed stable in the thermodynamic limit  $L \rightarrow \infty$  and that the element accountable for this stability is the procedure used to calculate the majority, which includes the site to be updated (target site) in addition to its nearest neighbors. For sites in the bulk of the lattice, this procedure essentially specifies the criterion of update in case of a tie, i.e., in case there is no majority among the neighbors. In this case, the majority-vote variant used by Parisi et al. leaves the state of the agent untouched, whereas the most common variant used in the literature sets that state at random with probability  $1/2$  [18, 19]. It should be noted, however, that the criterion used by Parisi et al. is actually the original definition of the majority-vote model as introduced in Refs. [16, 17]. It is surprising that such (apparently) minor implementation detail produces nontrivial consequences in the thermodynamic limit, which can actually be confirmed analytically using a mean-field approach that takes into account the correlation between nearest neighbors – the pair approximation [12]. However, the addition of a thermal-like noise such that the individuals may take a stance opposed to the majority opinion with some small probability destabilizes the globally polarized regime leading to one of the two low-temperature homogeneous steady states of the Ising model [20]. In that sense we disagree with the claim by Parisi et al. that their variant of the majority-vote model is more robust than Axelrod’s model to the effect of this type of noise.

The rest of this paper is organized as follows. In Sect. II we describe the variant of the majority-vote model proposed by Parisi et al., which henceforth we refer to as the extended majority-vote model since its key ingredient is the stretching of the neighborhood to include the target site [15]. In Sect. III we present the mean-field approach to this model using the single-site and pair approximations [12, 18]. In Sect. IV we use extensive Monte Carlo simulations to investigate several properties of the absorbing configurations such as the average number of opinion domains or clusters, the size of the largest cluster and the distribution of cluster sizes, giving emphasis to their dependences on the lattice size. In that section also we discuss the vulnerability of the heterogeneous opinion regime against a thermal-like noise, which allows the individuals to disagree with the majority opinion. Finally, in Sect. V we present our concluding remarks.

## II. MODEL

The agents are fixed at the sites of a square lattice of size  $L \times L$  with open boundary conditions (i.e., agents at the corners interact with two neighbors, agents at the sides with three, and agents in the bulk with four nearest neighbors). The initial configuration is random: the opinion of each agent is set by a random digit 0 or 1 with equal probability. At each time we pick a target agent at random and then verify which is the more frequent opinion (1 or 0) among its extended neighborhood, which includes the target agent itself. The opinion of the target agent is then changed to match the corresponding majority value. We note that there are no ties for agents in the bulk or at the corners of the square lattice since in these cases the extended neighborhood comprises 5 and 3 sites, respectively. However, agents at the sides of the lattice have an extended neighborhood of 4 sites (i.e., 3 neighbors plus the target agent) and so in case of a tie, the opinion of the target agent remains unchanged. Of course, in the limit of large lattices the contribution of these boundary sites will be negligible. This procedure is repeated until the system is frozen in an absorbing configuration.

Although the majority-vote rule or, more generally, the frequency bias mechanism for opinion change [3] is a homogenizing assumption by which the agents become more similar to each other, the above-described model does seem to exhibit global polarization, i.e., heterogeneous absorbing configurations [15]. Since the study of Ref. [15] was based on a small lattice of linear size  $L = 20$  a more careful analysis is necessary to confirm whether this conclusion holds in the thermodynamic limit as well. It is interesting to note that for the more popular variant of the majority-vote model, in which the state of the target site is not included in the majority reckoning, and ties are decided by choosing the opinion of the target agent at random with probability  $1/2$ , the only absorbing states in the thermodynamic limit are the two homogeneous configurations. For finite lattices, however, we find heterogeneous absorbing configurations characterized by stripes that sweep the entire lattice. In Sect. IV we carry out a finite size scaling analysis of the extended majority-vote rule aiming at understanding the nature of the opinion domains that fragment the absorbing configurations.

## III. MEAN-FIELD ANALYSIS

In this section we offer an analytical approximation to the extended majority-vote model introduced by Parisi et al [15]. The state of the agent at site  $i$  of the square lattice is represented by the binary variable  $\eta_i = 0, 1$  and so the configuration of the entire lattice comprising  $N = L^2$  sites is denoted by  $\eta \equiv (\eta_1, \eta_2, \dots, \eta_N)$ . The master equation that governs the time evolution of the

probability distribution  $P(\eta, t)$  is given by

$$\frac{d}{dt}P(\eta, t) = \sum_i [W_i(\tilde{\eta}^i) P(\tilde{\eta}^i, t) - W_i(\eta) P(\eta, t)] \quad (1)$$

where  $\tilde{\eta}^i = (\eta_1, \dots, 1 - \eta_i, \dots, \eta_N)$  and  $W_i(\eta)$  is the transition rate between configurations  $\eta$  and  $\tilde{\eta}^i$  [18, 19]. For the extended majority-vote model we have

$$W_i(\eta) = \left| \Theta \left[ \sum_{\delta} \eta_{i+\delta} + \eta_i - 3 \right] - \eta_i \right| \quad (2)$$

where the notation  $\sum_{\delta}(\dots)$  stands for the sum over the 4 nearest neighbors of site  $i$  and  $\Theta(x) = 1$  if  $x \geq 0$  and 0 otherwise.

We are interested in determining the fraction of agents holding opinion 1 or, equivalently, the fraction of sites in state 1, which we denote by  $\rho$ . Since all sites are equivalent we have  $\rho \equiv \sum_i \eta_i / N = \langle \eta_i \rangle$  and this mean value is given by the equation

$$\frac{d}{dt} \langle \eta_i \rangle = \langle (1 - 2\eta_i) W_i(\eta) \rangle \quad (3)$$

with  $\langle (\dots) \rangle \equiv \sum_{\eta} (\dots) P(\eta, t)$  as usual. To carry out this average we need to make approximations. In what follows we study in detail two such approximation schemes, namely, the single-site approximation and the pair approximation.

#### A. The single-site approximation

This is the simplest mean-field scheme which assumes that the sites are independent random variables so that Eq. (3) becomes

$$\begin{aligned} \frac{d\rho}{dt} = & -\rho \sum_{n=0}^4 B_n^4(\rho) |\Theta[n-2] - 1| \\ & + (1 - \rho) \sum_{n=0}^4 B_n^4(\rho) \Theta[n-3] \end{aligned} \quad (4)$$

where  $B_n^m$  is the Binomial distribution

$$B_n^m(\rho) = \binom{m}{n} \rho^n (1 - \rho)^{m-n}. \quad (5)$$

Carrying out the sums explicitly and rearranging the terms yield

$$\frac{d\rho}{dt} = -\rho(1 - \rho)(2\rho - 1)(3\rho^2 - 3\rho - 1). \quad (6)$$

This equation, which is invariant to the change  $\rho \leftrightarrow 1 - \rho$ , has three fixed points, namely,  $\rho^* = 0$ ,  $\rho^* = 1$  and  $\rho^* = 1/2$ . The first two fixed points are stable and the third one is unstable. This means that in the single-site approximation the only stable configurations are the homogeneous ones. Finally, we note that  $\rho$  contains the same information as the single-site probability distribution  $p_1(\eta_i)$ . In fact,  $p_1(\eta_i = 1) = \rho$  and  $p_1(\eta_i = 0) = 1 - \rho$ .

#### B. The pair approximation

In this scheme we assume that nearest neighbors sites are statistically dependent random variables so that, in addition to the single-site probability distribution  $p_1(\eta_i)$ , we need to compute the pair probability distribution  $p_2(\eta_i, \eta_{i+\delta})$  as well. Of particular importance for the subsequent calculations is the conditional probability distribution  $p_{1|1}(\eta_{i+\delta} | \eta_i)$  which is given simply by the ratio between the pair and the single-site probability distributions.

For the sake of concreteness, let us denote the states of the 4 neighbors of site  $i$  by  $\eta_1, \eta_2, \eta_3$  and  $\eta_4$ . These are independent random variables in the pair approximation since they are not nearest neighbors in the square lattice, so the sum  $n = \eta_1 + \eta_2 + \eta_3 + \eta_4$  that appears in the argument of the Theta functions is a sum of independent variables. With these notations we can rewrite Eq. (3) as

$$\begin{aligned} \frac{d\rho}{dt} = & -\rho \sum_{\eta_1, \dots, \eta_4} p_{4|1}(\eta_1, \eta_2, \eta_3, \eta_4 | 1) |\Theta(n-2) - 1| \\ & + (1 - \rho) \sum_{\eta_1, \dots, \eta_4} p_{4|1}(\eta_1, \eta_2, \eta_3, \eta_4 | 0) \Theta(n-3) \end{aligned} \quad (7)$$

where we have carried out the sum over  $\eta_i = 0, 1$  explicitly. The assumption that  $\eta_1, \dots, \eta_4$  are statistically independent random variables allows to write

$$p_{4|1}(\eta_1, \eta_2, \eta_3, \eta_4 | \eta_i) = p_{1|1}(\eta_1 | \eta_i) \times \dots \times p_{1|1}(\eta_4 | \eta_i) \quad (8)$$

and finally obtain

$$\begin{aligned} \frac{d\rho}{dt} = & -\rho \sum_{n=0}^4 B_n^4[p_{1|1}(1 | 1)] |\Theta[n-2] - 1| \\ & + (1 - \rho) \sum_{n=0}^4 B_n^4[p_{1|1}(1 | 0)] \Theta[n-3] \end{aligned} \quad (9)$$

which is identical to Eq. (4) except for the arguments of the binomial distributions. Using the notation  $\phi \equiv p_2(1, 1)$  we write

$$p_{1|1}(1 | 1) = \frac{\phi}{\rho} \quad (10)$$

$$p_{1|1}(1 | 0) = \frac{\rho - \phi}{1 - \rho} \quad (11)$$

so that Eq. (9) involves only two unknowns,  $\rho$  and  $\phi$ . Carrying out the summations explicitly so as to eliminate the Theta functions yields

$$\begin{aligned} \frac{d\rho}{dt} = & -\rho \left[ B_0^4\left(\frac{\phi}{\rho}\right) + B_1^4\left(\frac{\phi}{\rho}\right) \right] \\ & + (1 - \rho) \left[ B_3^4\left(\frac{\rho - \phi}{1 - \rho}\right) + B_4^4\left(\frac{\rho - \phi}{1 - \rho}\right) \right] \end{aligned} \quad (12)$$

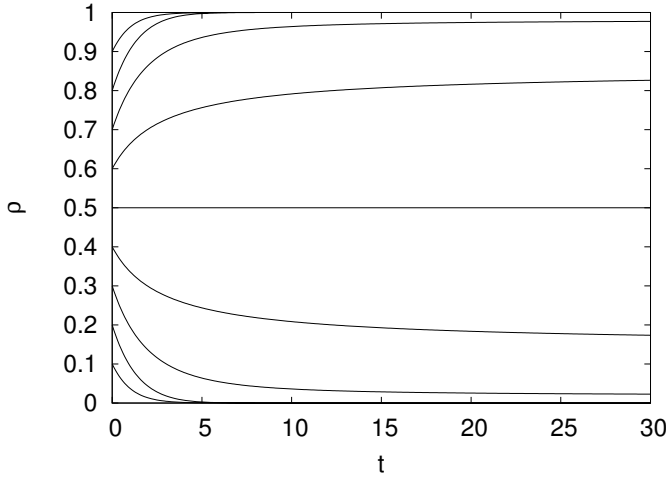


FIG. 1: Time evolution of the fraction of sites in state 1,  $\rho$ , in the pair approximation obtained by solving Eqs. (12) and (15) using Euler's method with step-size 0.01 for different initial conditions (bottom to top)  $\rho_0 = 0.1, \dots, 0.9$ .

We note that this equation reduces to Eq. (6) in the case the neighboring sites are assumed independent, i.e.,  $\phi = \rho^2$ .

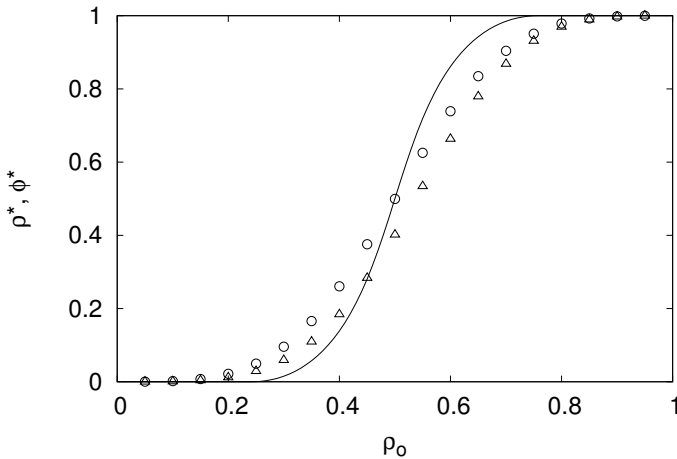


FIG. 2: The fraction of sites in state 1 at equilibrium,  $\rho^*$  (represented by  $\circ$ ), and the probability that two neighbors are in state 1 at equilibrium,  $\phi^*$  (represented by  $\triangle$ ) as functions of the initial fraction of sites in state 1,  $\rho_0$ . The solid line is the result of the pair approximation for which  $\phi^* \rightarrow \rho^*$ . The initial condition is  $\rho = \rho_0$  and  $\phi = \rho_0^2$ . The symbols show the results of the Monte Carlo simulations for a square lattice of linear size  $L = 200$ .

Next, our task is to determine an equation for  $\phi = \langle \eta_i \eta_j \rangle$  where  $j$  labels one of the four nearest neighboring sites of  $i$ . We have

$$\frac{d}{dt} \langle \eta_i \eta_j \rangle = 2 \langle \eta_j (1 - 2\eta_i) W_i(\eta) \rangle. \quad (13)$$

Carrying out the average over  $\eta_i$  and  $\eta_j$  (say  $j = 1$ )

explicitly yields

$$\begin{aligned} \frac{d\phi}{dt} = & -2\rho p_{1|1} (1|1) \sum_{m=0}^3 B_m^3 [p_{1|1} (1|1)] |\Theta[m-1] - 1| \\ & + 2(1-\rho) p_{1|1} (1|0) \sum_{m=0}^3 B_m^3 [p_{1|1} (1|0)] \Theta[m-2] \end{aligned} \quad (14)$$

which can be written more compactly as

$$\begin{aligned} \frac{d\phi}{dt} = & -2\phi B_0^3 \left( \frac{\phi}{\rho} \right) \\ & + 2(\rho - \phi) \left[ B_2^3 \left( \frac{\rho - \phi}{1 - \rho} \right) + B_3^3 \left( \frac{\rho - \phi}{1 - \rho} \right) \right]. \end{aligned} \quad (15)$$

Equations (12) and (15) determine completely the time evolution of  $\rho$  and  $\phi$  and so they are our final equations for the pair approximation of the extended majority-vote model. Figure 1, which shows the time evolution of the density of sites in state 1, confirms that Eq. (15) is indeed invariant to the change  $0 \leftrightarrow 1$ . Most surprisingly, this figure uncovers an unexpected dependence on the choice of the (random) initial condition  $\rho_0$  and  $\phi_0 = \rho_0^2$ : indeed in the range  $\rho_0 \in (\rho_m, 1 - \rho_m)$ , where  $\rho_m \approx 0.25$ , the equilibrium solution  $\rho^*$  is a smooth function of  $\rho_0$ , i.e., there is a continuum of fixed points. Accordingly, Fig. 2 shows the fixed point solutions of Eqs. (12) and (15) for the usual situation in which the states of the sites of the initial configuration are set 1 with probability  $\rho_0$  and 0 with probability  $1 - \rho_0$ . For this setting we have  $\phi_0 = \rho_0^2$ .

The mathematical explanation for the odd dynamical behavior exhibited in Figs. 1 and 2 is that the dynamic evolution is such that  $\rho \rightarrow \phi$  for  $t \rightarrow \infty$ , a condition that solves the two equations (12) and (15) at equilibrium (i.e.,  $d\rho/dt = d\phi/dt = 0$ ) simultaneously and so leaves one of the unknowns free to take any arbitrary value set by the dynamics or the initial conditions. The physical reason is that there are in fact many absorbing configurations very close to the random initial configurations and a few lattice updates (typically 10) is sufficient to freeze the dynamics (see Fig. 3). In fact, the comparison with the results of the Monte Carlo simulations exhibited in Fig. 2 shows a good qualitative agreement between the pair approximation and the simulation results.

Finally, we note that the pair approximation for the variant of the majority-vote model in which ties are decided by flipping the state of the target site with probability  $1/2$  yields the anticipated result that the only stable fixed points are  $\rho = \phi = 0$  and  $\rho = \phi = 1$ , whose basins of attraction depend on whether  $\rho_0$  is less or greater than  $1/2$ .

#### IV. MONTE CARLO SIMULATIONS

In this section we first demonstrate that the heterogeneous absorbing configurations of the extended majority-

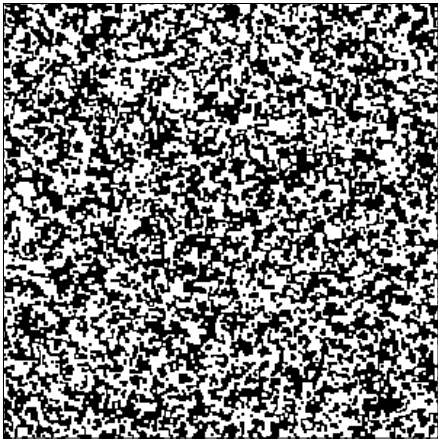


FIG. 3: A typical absorbing configuration of the extended majority-vote model for a lattice of linear size  $L = 300$ . Agents with opinion 1 are painted black and agents with opinion 0 are painted white. There are a total of  $M = 779$  clusters and the largest one comprises  $S_m = 4581$  agents.

vote model do persist in the thermodynamic limit and then we proceed with the characterization of the opinion domains (clusters) that fragment those configurations. Figure 3 illustrates one such a configuration for  $L = 300$ . We recall that a cluster is simply a connected, bounded lattice region wherein the agents share the same opinion. We focus on a few relevant statistical quantities to characterize the cluster organization, namely, the average number of clusters  $\langle M \rangle$ , the average size of the largest cluster  $\langle S_m \rangle$ , and the distribution of cluster sizes  $P_S$ . We must evaluate these quantities for different lattice sizes (typically we use  $10^4$  samples for each  $L$ ) and then take an appropriate extrapolation procedure to infinite lattices ( $L \rightarrow \infty$ ).

To simulate efficiently the extended majority-vote model for large lattices we first make a list of the active agents. An active agent is an agent whose opinion differs from the most frequent opinion among its extended neighborhood. Clearly, only active agents can change their opinions and so it is more efficient to select the target agent randomly from the list of active agents rather than from the entire lattice. In the case that the opinion of the target agent is modified by the majority-vote rule, we need to re-examine the active/inactive status of the target agent as well as of all its neighbors so as to update the list of active agents. The dynamics is frozen when the list of active agents is empty. The implementation of a similar procedure allowed the simulation of Axelrod's model for very large lattices and the clarification of several issues regarding the stability of the heterogeneous absorbing configurations of that model [14, 21].

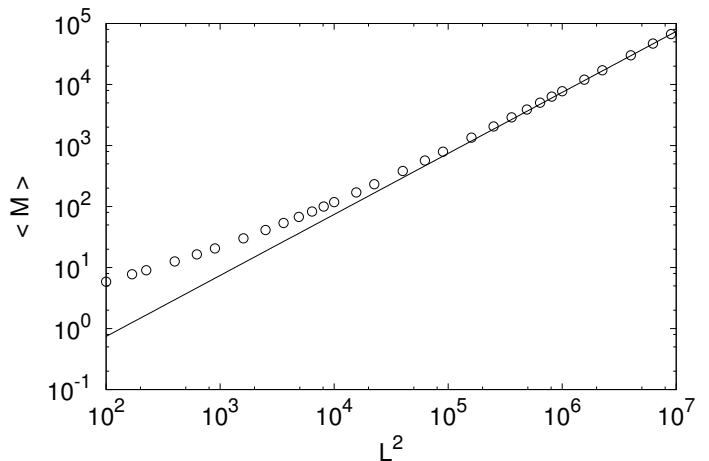


FIG. 4: Logarithmic plot of the average number of clusters  $\langle M \rangle$  as function of the the lattice area  $L^2$ . The solid straight line is the fitting  $\langle M \rangle = 0.00742L^2$  for large  $L$ . Each symbol represents the average over  $10^4$  samples so the sizes of the error bars are smaller than the symbol sizes.

#### A. Statistics of the number of clusters

We begin our analysis by presenting the dependence of the average number of clusters  $\langle M \rangle$  on the lattice area  $L^2$  in Fig. 4. The increase of  $\langle M \rangle$  with increasing  $L^2$  is the evidence that confirms that the extended majority-vote model exhibits heterogeneous absorbing configurations in the thermodynamic limit,  $L \rightarrow \infty$ . More to the point, we find

$$\lim_{L \rightarrow \infty} \frac{\langle M \rangle}{L^2} = 0.00742 \pm 10^{-5}. \quad (16)$$

For the purpose of comparison, for frozen random configurations in which the  $L^2$  sites are set to 1 or 0 with the same probability this ratio yields  $0.1342 \pm 0.0001$  (and so the average number of clusters scales linearly with the lattice area too). We note that the reciprocal of the ratio given in Eq. (16) is the average size of the clusters:  $\langle S \rangle \approx 134.8$  for the extended majority-vote model and  $\langle S \rangle \approx 7.45$  for random configurations.

#### B. Statistics of the largest cluster

Although the mean size of a typical cluster is finite, there may be clusters whose sizes can become arbitrarily large as the lattice size increases. To investigate this point we show in Fig. 5 the average size of the largest cluster  $\langle S_m \rangle$  as function of the lattice area. As in the case of  $\langle M \rangle$ , the asymptotic scaling is revealed only for large lattices ( $L > 500$ ) and it indicates that  $\langle S_m \rangle$  increases with  $\ln L^2$  for large  $L$ .

In the thermodynamic limit the relevant quantity is

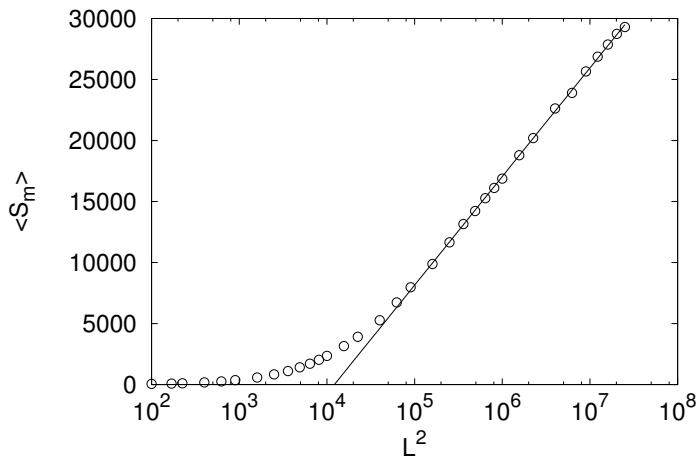


FIG. 5: The average size of the largest cluster  $\langle S_m \rangle$  as function of the the lattice area  $L^2$ . The solid line is the fitting  $\langle S_m \rangle = 1933 \ln L^2 - 36363$ . Note the logarithmic scale in the  $x$ -axis.

then

$$\lim_{L \rightarrow \infty} \frac{\langle S_m \rangle}{\ln L^2} = 1933 \pm 10. \quad (17)$$

We found that  $\langle S_m \rangle$  scales with  $\ln L^2$  for random configurations also, though the ratio  $\lim_{L \rightarrow \infty} \langle S_m \rangle / \ln L^2 = 53.0 \pm 0.2$  is considerably smaller than the ratio given in Eq. (17).

It is interesting to note that the standard deviation  $[\langle S^2 \rangle - \langle S \rangle^2]^{1/2}$  tends to the constant value  $695.5 \pm 0.5$  in the thermodynamic limit. This amounts to a large but finite variance and so in order to satisfy the Tchebycheff inequality the set of clusters whose size grows like  $\ln L^2$  must have measure zero in that limit. Since the probability that a randomly chosen site belongs to one such a cluster vanishes like  $(\ln L) / L^2$ , the measure of the set of diverging clusters will be vanishingly small if its cardinality is finite, i.e., if only a finite number of clusters have sizes scaling with  $\ln L^2$ .

### C. Distribution of cluster sizes

Up to now we found no qualitative differences between the statistical properties of the clusters produced by the extended majority-vote rule or by assigning randomly the digits 1 and 0 to the sites of the square lattice. In fact, for both types of configurations the quantities  $\langle M \rangle$  and  $\langle S_m \rangle$  exhibit the same scaling behavior with the lattice area  $L^2$ . However, a more detailed view of the cluster organization is given by the distribution  $P_S$  of cluster sizes  $S$ , which is shown in Fig. 6 for different lattice sizes. The data seems to be remarkably well fitted by the power-law distribution  $P_S \sim S^{-1.5}$  for over more than three decades. In addition, the figure indicates that the region where

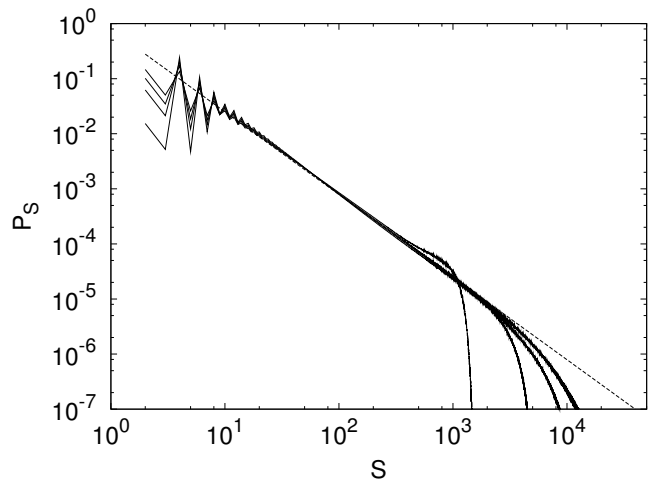


FIG. 6: Logarithmic plot of the distribution of cluster sizes  $S$  for (solid lines from left to right at  $P_S = 10^{-6}$ )  $L = 50, 100, 200$  and  $1000$ . The dashed straight line is the fitting  $P_S = 0.79 S^{-1.5}$ . These distributions are obtained by sampling  $10^7$  absorbing configurations of the extended majority-vote model.

the power-law fitting holds increases with increasing  $L$ . This power-law distribution, however, is not compatible with our previous findings of finite values for the mean and variance of  $P_S$ , since the distribution  $P_S \sim S^{-1.5}$  has infinite mean and variance.

To answer this conundrum, in Fig. 7 we plot the same data using a semi-logarithmic scale instead of the log-log scale of Fig. 6. The results show that for large lattice sizes the distribution  $P_S$  is in fact exponential, the power-law behavior being valid only in an intermediate range of cluster sizes. The results for the larger lattice  $L = 1000$  (though not the results for the smaller lattices  $L = 50$  and  $L = 100$ ) show that the exponential distribution is not a mere cut-off inherent to the finitude of the lattices used in the simulations, as manifested by the straight-line appearance of  $P_S$  revealed by the semi-log graph in the regime of large clusters. For the sake of comparison, in Fig. 8 we show the distribution of cluster sizes for frozen random configurations which can be well-described by the exponential distribution  $P_s \approx 0.00085 \exp(-0.02S)$  for large  $S$ . The puzzling power-law behavior found for intermediate values of  $S$  in the extended majority-vote model is missing in this case.

Finally, it is interesting to note that, for any absorbing configuration of the extended majority-vote model, clusters of size 1 are prohibited, clusters of sizes 2 and 3 are allowed at the sides of the square lattice only, and the only cluster of size 4 allowed in the bulk of the lattice is that in which the four sites surrounding a unit cell are in the same state. In fact, this elementary square cluster is the only structure capable to propagate through the lattice, i.e., whenever a stable cluster is formed one such elementary square is formed.

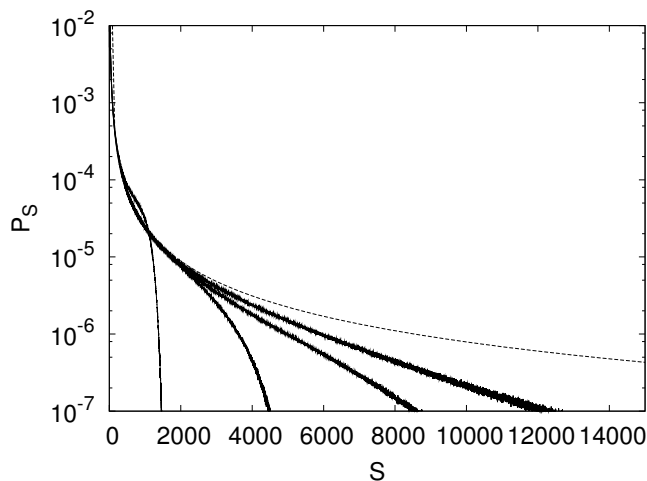


FIG. 7: The same data shown Fig. 6 plotted using a semi-logarithmic scale.

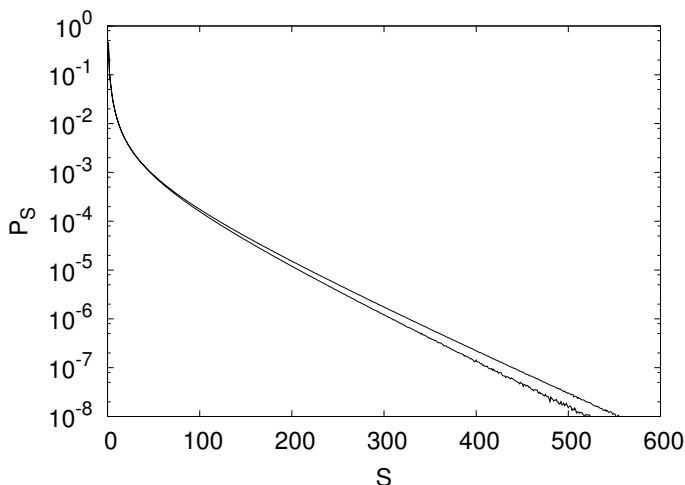


FIG. 8: Semi-logarithmic plot of the distribution of cluster sizes  $S$  for random configurations with (solid lines from bottom to top)  $L = 100$  and  $300$ . These distributions are obtained through the sampling of  $10^8$  random configurations.

#### D. Vulnerability to noise

A word is in order about the robustness of the heterogeneous absorbing configurations to the effect of noise, which allows the agents to oppose the opinion of the majority with some small probability. More pointedly, after applying the update rule for each agent, which may or may not result in the change of its opinion, we flip its opinion with probability  $p \in [0, 1/2]$  [19]. Since in this case there are no absorbing configurations the notion of active sites is useless and so we implement the dynamics by picking lattice sites at random with the same probability. Then the unit of time (a Monte Carlo step) corresponds to the update of  $L^2$  randomly chosen sites. For

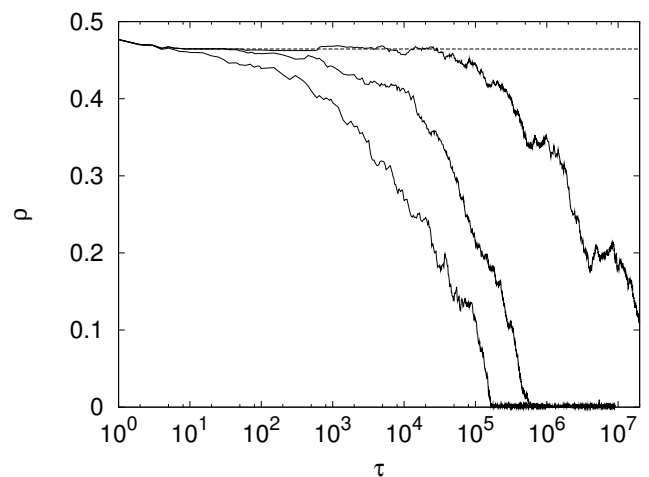


FIG. 9: Fraction of sites in state 1 as function of the number of Monte Carlo steps  $\tau$  for the thermal noise intensity (solid lines from left to right)  $p = 10^{-3}, 10^{-4}$  and  $10^{-5}$  and for a lattice of size  $L = 50$ . The dashed line is the evolution for the noiseless case which rapidly gets stuck in an absorbing configuration. The initial configuration is the same for the four trajectories.

$L = 50$  we present in Fig. 9 the time evolution of the fraction of sites in state 1, which we denote by  $\rho$  as in Sect. III, for different values of the noise parameter  $p$  but for the same initial configuration. This figure, which exhibits the evolution of a single sample, shows the vulnerability of the heterogeneous absorbing configurations against a vanishingly amount of thermal noise if one gives enough time for thermalization. For the small values of  $p$  considered, the steady-state is close to one of the two homogeneous configurations, with all individuals exhibiting opinion 0 or opinion 1. The specific outcome is a stochastic process which depends on the choice of the initial configuration as well as on the sequence of random numbers used in the update rule.

## V. CONCLUSION

This paper is motivated by the claim that the extended majority-vote model, for which the target site counts in the reckoning of the majority, exhibits a nontrivial multicultural regime, i.e., heterogeneous absorbing configurations [15]. From the perspective of the statistical physics, we find this claim most intriguing, as we expect the model to behave similarly to the majority-vote models commonly considered in the physics literature, which are basically Ising models with zero-temperature Glauber kinetics [20], and so exhibit only two homogeneous absorbing configurations in the thermodynamic limit. Our first impression was that the heterogeneous absorbing configurations were artifacts of the small lattice size ( $L = 20$ ) used or of some ‘non-physical’ elements of the original model such as the nearest and next-nearest neighbors in-

teractions (Moore neighborhood) and the parallel update of the sites [15].

Accordingly, we have modified the original model proposed by Parisi et al. by introducing the usual nearest neighbors interactions (von Neumann neighborhood) and the random sequential update of sites. A careful finite size scaling analysis of a few relevant measures that characterize the absorbing configurations shows that the heterogeneous absorbing configurations not only persist in the thermodynamic limit but produce a tricky distribution of cluster sizes  $P_S$  that decays as a power law  $P_S \sim S^{-1.5}$  for clusters of intermediate size  $S$  and as an exponential for very large clusters sizes (see Figs. 6 and 7). Essentially, the reason for this somewhat unexpected outcome is the criterion of update in case of a tie for a site in the bulk of the lattice: the site remains unchanged rather than flipping to another state with probability  $1/2$  as usually done in statistical mechanics models [18, 19]. What is remarkable is that the existence of these heterogeneous absorbing configurations for the extended majority-vote model, as well as their absence in the more usual variants of that model, can actually be predicted analytically using the pair approximation: the multiple-clusters regime is signaled by the presence of an infinity of attractive fixed points of the mean-field equations.

We found that the statistical properties (e.g., average number of clusters, mean size of the largest cluster and the asymptotic distribution of cluster sizes) of the clusters that break up the absorbing configurations (see Fig. 3) are qualitatively identical to those of random configurations. This could also be inferred by the very short convergence times (see dashed line in Fig. 9) which indicate that the absorbing configurations are very close to the initial random configurations, since a few lattice updates suffice to reach them. We are not aware of any similar study of the statistical properties of the heterogeneous configurations of Axelrod's model, so we cannot compare the cluster organization of these two models.

Our findings, which corroborate the results of Parisi et al. [15], shows that the extended majority-vote model does exhibit a 'multicultural' regime, despite the fact that the update rule biases the agents to become more similar to each other. A similar conclusion holds for Axelrod's model as well [6, 13, 14], except that in Axelrod's model the similarity is a prerequisite for interactions - the 'birds of a feather flock together' hypothesis which states that individuals who are similar to each other are more likely to interact and then become even more similar [2]. (A similar assumption has been used to model the interspecies interactions in spin-glass like model ecosystem [22].) The majority-vote model is considerably simpler and converges to the absorbing configurations much faster than Axelrod's. However, the (short) inventory of advantages stops here: in disagreement with the claim of Parisi et al. [15] we found that the absorbing configurations of the extended majority-vote model are vulnerable to the noisy effect of flipping the opinions of the agents with some small probability. It is well-known that this type of noise destabilizes the heterogeneous configurations of Axelrod's model too [8]. Of course, the extended majority-vote model lacks the main appealing feature of Axelrod's model, namely, the existence of a non-equilibrium phase transition that separates the homogeneous and the polarized regimes in the thermodynamic limit. In that sense it would be interesting to find out how a similar transition could be induced in the zero-temperature majority-vote model.

### Acknowledgments

This research was supported by The Southern Office of Aerospace Research and Development (SOARD), grant FA9550-10-1-0006, and Conselho Nacional de Desenvolvimento Científico e Tecnológico (CNPq).

- 
- [1] B. Latané, *American Psychologist* **36**, 343 (1981).
  - [2] S. Moscovici, *Handbook of Social Psychology* **2**, 347 (1985).
  - [3] R. Boyd and P. J. Richerson, *Culture and the evolutionary process* (University of Chicago Press, Chicago, 1985).
  - [4] A. Nowak, J. Szamrej and B. Latané, *Psychol. Rev.* **97**, 362 (1990).
  - [5] C. Castellano, S. Fortunato and V. Loreto, *Rev. Mod. Phys.* **81**, 591 (2009).
  - [6] R. Axelrod, *J. Conflict Res.* **41**, 203 (1997).
  - [7] J. Kennedy, *J. Conflict Res.* **42**, 56 (1998).
  - [8] K. Klemm, V. M. Eguíluz, R. Toral, M. San Miguel, *Phys. Rev. E* **67**, 045101R (2003).
  - [9] J. M. Greig, *J. Conflict Res.* **46**, 225 (2002).
  - [10] K. Klemm, V. M. Eguíluz, R. Toral, M. San Miguel, *Physica A* **327**, 1 (2003).
  - [11] K. Klemm, V. M. Eguíluz, R. Toral, M. San Miguel, *Phys. Rev. E* **67**, 026120 (2003).
  - [12] J. Marro and R. Dickman, *Nonequilibrium Phase Transitions in Lattice Models* (Cambridge University Press, Cambridge, UK, 1999).
  - [13] C. Castellano, M. Marsili and A. Vespignani, *Phys. Rev. Lett.* **85**, 3536 (2000).
  - [14] L. A. Barbosa and J. F. Fontanari, *Theory Biosci.* **128**, 205 (2009).
  - [15] D. Parisi, F. Cecconi, F. Natale, *J. Conflict Res.* **47**, 163 (2003).
  - [16] T. M. Liggett, *Interacting Particle Systems* (Springer, New York, 1985).
  - [17] L. Gray, in *Particle systems, random media, and large deviations* (American Mathematical Society, Providence, RI, 1985), Vol. 41, pp. 149–160.
  - [18] T. Tomé, M. J. de Oliveira and M. A. Santos, *J. Phys. A: Math. Gen.* **24** 3677 (1991).
  - [19] M. J. de Oliveira, *J. Stat. Phys.* **66**, 273 (1992).
  - [20] R. J. Glauber, *J. Math. Phys.* **4**, 294 (1963).



- [21] L. R. Peres and J. F. Fontanari, *J. Phys. A: Math. Theor.* **43**, 055003 (2010). **89**, 148101 (2002).
- [22] V. M. de Oliveira and J. F. Fontanari, *Phys. Rev. Lett.*